2019 International Conference on Robotics and Automation (ICRA)
Palais des congres de Montreal, Montreal, Canada, May 20-24, 2019

Differentially-Clutched Series Elastic Actuator for Robot-Aided Musculoskeletal Rehabilitation

Brayden DeBoon, Scott Nokleby, Nicholas La Delfa, and Carlos Rossa

Abstract— **Series elastic actuators have proven to be an elegant response to the issue of safety around human-robot interaction. The compliant nature of series elastic actuators provides the potential to be applied in robot-aided rehabilitation for patients with upper and lower limb musculoskeletal injuries. This paper proposes a new series elastic actuator to be used in robot-aided musculoskeletal rehabilitation. The actuator is composed of a DC motor, a torsion spring, and a magnetic particle brake coupled to one common output shaft through a differential gear. The proposed topology focuses on three types of actuation modes most commonly used in rehabilitation, i.e., free motion, elastic, and assistive/resistive motion. A dynamic model of the actuator is presented and validated experimentally and the ability of the actuator to follow a reference torque is shown in different experimental scenarios.**

I. Introduction

The rise of collaborative robotic systems is leading to a paradigm shift in robotics. The robotic systems of today are moving away from confined industrial settings and making their way into more complex environments, such as homes or hospitals, to work alongside humans to complement our natural capabilities. This shift introduces a number of challenges with regard to the safety of human-robot interaction. Anytime there is a possibility for a human to come in close proximity to a robot, the number one condition for the choice of actuation method should depend solely on safety [1]. There is a growing need for high-performance actuators with respect to safety in a multitude of fields as human-robot interaction has become more prominent, deriving from efforts to increase productivity, efficiency, safety, and convenience to the general public. Potential fields for compliant actuators include haptics, manufacturing, shipping, automotive, retail, service, and in the medical field for uses such as rehabilitation or surgery.

Traditionally, collaborative robots implement force sensors at one or more joints, however, these sensors are expensive and rely on software to guarantee compliance [2]–[4]. An alternative approach to the use of force sensors comes in the form of Series Elastic Actuators (SEAs). Series elastic actuators are devices that control motion in robotic systems using an elastic component to measure forces as well as provide a mechanical means of guaranteeing compliance by decoupling the actuator dynamics to the user with the introduction of a spring [5].

A critical scenario in which safety is paramount is robot-assisted rehabilitation. Two common examples where compliant robots can aid in the recovery process while ensuring safety is in neurological and musculoskeletal rehabilitation. While the SEA concept has been applied to single purpose neurological rehabilitation devices [6], [7], most of these actuators lack the performance requirements to be implemented in devices capable of addressing the multiple phases of musculoskeletal rehabilitation [8]. These phases address the differing requirements between assisting a patient in range of motion recovery and strengthening the injured area using a resistive approach. There has been limited effort to combine these traits for collaborative rehabilitation robots.

An actuator to be used in rehabilitation devices must satisfy three major operating modes that are coupled to different stages of rehabilitation. The first mode entails that the device has to be able to become fully compliant at a moments notice, allowing the patient to move the device freely with little effort [9]. The second operating mode is patient assistance. This is the stage of rehabilitation in which a patient is unable to achieve a full range of motion about a single or multiple joints due to an impeding inability to perform coordinated motion. The actuator must provide a reasonable amount of force to assist the patient in accomplishing a particular task that they would otherwise not be able to complete on their own. The third mode is resistive mode; once the patient has regained their full range of motion, the injured area must then be strengthened back to as close to the pre-injured state as possible [10]. This requires the device to oppose the motion provided by the patient and dissipate the applied energy in a safe and controlled manner, as well as possess the ability to increase in difficulty as the patient progresses [11].

The rehabilitation devices containing the actuators should be versatile enough to take the form of a range of rehabilitation technologies currently in practice at clinics, from mimicking a simple elastic band to providing precise assistance in completing a complex movement. There has been a number of attempts to fully optimize the ability of an actuator to provide the performance requirements mimicking conventional rehabilitation devices. Some of the characteristics expected from these devices include force bandwidth, efficiency, transparency, range of motion, size, weight, controllability, and patient comfort. The most common actuator topologies used in literature are shown in Fig. 1. Many of the actuators in the figure make use of a motor and either a brake or clutch coupled with a spring in various arrangements.

B. DeBoon, S. Nokleby, and C. Rossa (corresponding author) are affiliated with the Faculty of Engineering and Applied Science, University of Ontario Institute of Technology, Oshawa, Ontario, Canada. E-mail: brayden.deboon@uoit.net; scott.nokleby@uoit.ca; carlos.rossa@uoit.ca.

N. La Delfa is affiliated with the Faculty of Health Sciences, University of Ontario Institute of Technology, Oshawa, Ontario, Canada. E-mail: nicholas.ladelfa@uoit.ca

978-1-5386-6026-3/19/$31.00 ©2019 IEEE

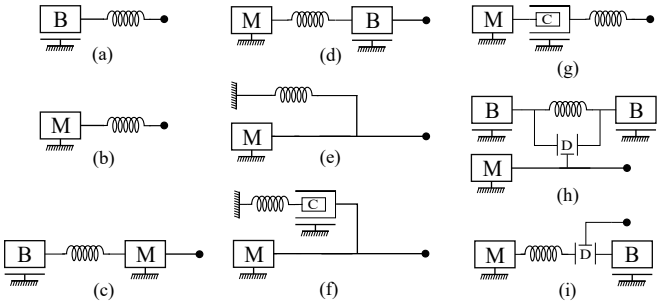

Fig. 1. Schematic of actuator topologies: Label M represents a motor assembly, B represents a braking mechanism, C represents a clutching mechanism, and D represents a differential. Coils represent elastic elements and the black circles represent the output.

The most basic version of an elastic actuator is shown in Fig. 1(a), which is a controllable brake in series with an elastic element. This topology demonstrates the basis of all elastic actuators: by controlling the amount of energy stored in the elastic element, one can effectively control or attenuate the forces at the output [12]. The actuator is strictly passive in this arrangement, where energy is either dissipated by the brake or stored in the spring. In order to achieve a greater range of forces an active element is introduced in place of the passive element as outlined in Fig. 1(b). This arrangement is a motor in series with an elastic component and was originally designed to partially decouple the end effectors dynamics to that of the motor, improve shock tolerances, force control, stability, and efficiency as compared to a rigidly connected motor with the main drawback of a reduced zero motion force bandwidth [5]. This arrangement is the most widely used in literature and with respect to robot-assisted rehabilitation to date [5], [13]–[22]. Since the introduction of elastic actuators, Conti, et al. [23] improved efficiency and safety by including a controllable brake, similar to the topology in Fig. 1(c). Bridging passive elements such as controllable brakes with elastic actuators provides another means of not only controlling the output force, but also the stored force within the actuator, significantly reducing the total power required to complete a movement and improving overall safety [23]. This gives elastic actuators the ability to switch between active and passive modes, making them suitable for rehabilitation of musculoskeletal disorders.

In an alternative arrangement shown in Fig. 1(d) [24], the brake and motor positions are swapped to increase the amount of output impedance thereby increasing the ability of the actuator to resist a patient's motion. However, in some circumstances motion in humans is better represented by the addition of a parallel spring similar to the arrangement shown in Fig. 1(e) [25]. The parallel spring allows for a more fluid and efficient energy transfer on repetitive motion tasks, especially when a limb is frequently halted and re-accelerated [26]. The spring connected in parallel limits the range of motion and hinders the ability to accommodate some phases of motion in which rapid stopping is necessary [27]. A solution to this issue proposed in [27] introduces a clutch to the elastic actuator as shown in Fig. 1(f). A clutch is traditionally defined as a device that has two states: one state allows the two bodies of the clutch to rotate independently, the other state locks the two bodies together such that the relative velocity is zero [28]. The clutch allows the actuator to engage or disengage an elastic element. Rouse, et al. [29] adapted this concept towards series elastic actuators (Fig. 1(g)) with the main advantage of tuning the actuators compliance using a series clutch to improve biomimicry and efficiency [29]. In fact, it has been shown that the force resolution of an actuator increases exponentially with the number of clutches and springs involved [30]. A recent approach, depicted in Fig. 1(h), makes use of a bi-directional clutched parallel elastic actuator that uses a differential spring-brake mechanism to decrease energy consumption and to control the energy is stored in the elastic element [31].

In this paper, the addition of a clutch to elastic actuators in the form of a differential clutch as presented in Fig. 1(i) is proposed. Differential clutches have the advantage of allowing three separate controllable bodies to rotate at different speeds. The use of a differential decreases the total mass of the actuator while maintaining functionality and compliance as compared to the addition of multiple clutch systems. In addition, a differential clutch adds a mode of redundancy to improve the safety of the actuator and reduces the amount of energy required to perform force control by including only a single low-power controllable device (differential clutch) over multiple clutches/brakes. Although differential clutches have been used in hybrid actuators [32], integrating differentials to elastic actuators has not been done. In this paper, the Differentially-Clutched Series Elastic Actuator (DC-SEA) is introduced. DC-SEA makes use of a differential clutch paired with an elastic-coupled DC motor and a magnetic particle brake as in Fig. 1(i). The main goal of the motor and brake working in tandem is to have the ability to couple the user shaft to a small-packaged motor with a high gear ratio, inevitably creating a slower response time, but maintaining the ability to completely decouple the user from the motor/spring pair in the event of an emergency. This provides two independently controlled mechanisms of safely decreasing the amount of energy either by using the motor to decompress the spring or by disengaging the brake, allowing for different operating modes as shown in Fig. 1.

In the DC-SEA topology, when a relatively high-gear ratio motor is powered off, this creates a pseudo-ground on one side of the elastic element creating a mode equivalent to that shown in Fig. 1(a). When the brake is fully engaged, the differential acts as a clutch between the output shaft and the motor-spring mechanism taking the form of Fig. 1(b). As opposed to traditional clutches such as those used in automobiles, the differential clutch can be used to continuously control the amount of force transferred between the output and the motor-spring assembly through the use of the magnetic particle brake, which can be considered to operate as a variable damper. The latter is able to fully recreate the functions of Fig. 1(g) and partially encompasses the capabilities of Fig. 1(c), (d), (f), and (h).

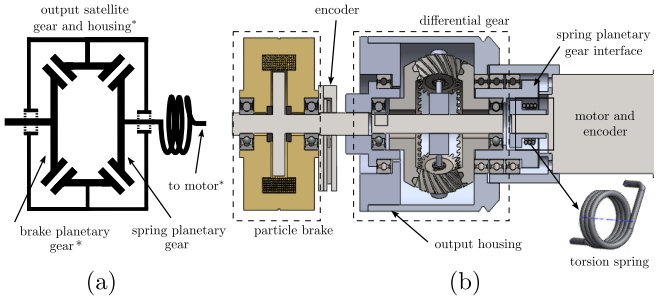

Fig. 2. (a) Drawing of the differential gear system. (b) CAD model cross section of the DC- SEA. The asterisk indicates an encoder-measured body.

II. Proof-of-Concept

A proof-of-concept DC-SEA was created adhering to the arrangement in Fig. 1(i). A model of the differential gear system is shown in Fig. 2(a). The outer/larger gears are defined as planetary gears and the smaller internal gears are satellite gears. A DC motor is coupled to one of the two planetary gears of the differential through a torsion spring assembly. The other planetary gear of the differential is coupled to a magnetic particle brake. There are three smaller satellite gears between the two planetary gears that are connected to the rotating output housing of the actuator as shown in Fig. 2(b). A spring assembly that mounts a series torsion spring between the motor and one of the planetary gears is described as the spring-planetary gear interface (see Fig. 2(b)). The output housing is rigidly connected to the satellite gears in the differential clutch, the housing itself acting as the output shaft. The output housing is coupled to an external encoder using a belt (not shown in Fig. 2). Two additional encoders with 2,048 pulses per revolution are used to measure the position of the brake and motor shafts.

The motor and encoder pair used in this actuator is a Cytron IG42E-24K with a 24:1 reduction gearbox with a nominal torque of 980 mNm with an encoder resolution of 480 pulses per rotation. The brake is a magnetic particle brake made by Placid Industries (B15-12-1) with a torque range of 34 mNm to 1,700 mNm.

The DC-SEA is able to achieve the following operating modes. The ***Free Motion*** mode is designed to allow the user to rotate the shaft freely. This is done by disengaging the brake and motor. Provided that the gearbox in the DC motor has a large reduction, the motors off-state torque translates to a fixed surface connected to one side of the torsional spring. If the user rotates the output shaft, all energy introduced to the actuator will be split between the brake and the torsional spring. In the ***Elastic Mode***, when the brake is engaged and the motor is static, the device is in an elastic state; as if the user is directly coupled to a grounded spring. The total energy stored in the spring can be controlled by adjusting the braking effort in the magnetic particle brake. In ***Active/Resistive Mode*** when both the motor and brake are engaged, the brake and differential act as a continuously variable-slip clutch between the motor-spring system and the end effector. The force transmitted to the end effector can be controlled by adjusting both the motor and braking effort in tandem. The motor can be used to compress the spring and engage the output shaft and both the motor and brake can decompress the spring to reduce the amount of stored energy, thus reducing the force applied to the end effector.

Each of these modes have applications in musculoskeletal rehabilitation. By controlling the commanded motor torque τ_{cm} and the commanded brake torque τ_{cb}, any of the above actuation modes can be achieved.

III. Equations of Motion

A schematic representation of the actuator dynamics is shown in Fig. 3. The sum of the torques about the motor shaft can be modelled by:

$$J_m\ddot{\theta}_m + b_m\dot{\theta}_m + k_s(\theta_m - \theta_s) = \tau_{cm}, \tag{1}$$

where τ_{cm} is the commanded motor torque, J_m is the moment of inertia about the motor shaft, and b_m is the damping coefficient of the motor. Throughout this paper, $\dot{\theta}$ and $\ddot{\theta}$ refer to the first and second time derivative of angular position θ, respectively. Subscript m refers to any parameter associated with the motor shaft. In addition to (1), the torque equations for the user, spring, and brake bodies of the differential are, respectively:

$$\tau_s + J_s\ddot{\theta}_s + b_s\dot{\theta}_s + b_d(\dot{\theta}_s - \dot{\theta}_b) + k_s(\theta_s - \theta_m) = 0 \tag{2}$$

$$\tau_u + \tau_{app} + J_u\ddot{\theta}_u + b_u\dot{\theta}_u = 0 \tag{3}$$

$$\tau_b + J_b\ddot{\theta}_b + b_b\dot{\theta}_b + b_d(\dot{\theta}_b - \dot{\theta}_s) + \tau_{cb} = 0, \tag{4}$$

where τ_s, τ_u, and τ_b are the torques of the spring, user, and brake bodies of the differential, respectively. Subscript u refers to parameters associated with the user differential body, subscript s and b relate to the spring and brake planetary gears in the differential, respectively. J_s, J_u, and J_b are the moments of inertia, and b_s, b_u, and b_b are the viscous friction components, b_d is the viscous friction coefficient between the satellite and planetary gears in the differential, $\ddot{\theta}_s$, $\ddot{\theta}_u$, and $\ddot{\theta}_b$ are the angular accelerations, $\dot{\theta}_s$, $\dot{\theta}_u$, and $\dot{\theta}_b$ are the angular velocities, θ_s, θ_u, and θ_b and are the angular positions about the planetary gear axis, k_s is the spring constant of the custom-made torsion spring, τ_{app} is the torque applied by the user, and τ_{cb} is the controlled braking torque of the magnetic particle brake. To model the actuator, the differential law of motion about $\dot{\theta}_s$ can be described as a function of the remaining velocity components: $\dot{\theta}_s = 2\dot{\theta}_u - \dot{\theta}_b$.

Considering the total power in the differential, coupled with efficiency coefficients η_u, η_s, and η_b to modulate for additional losses in the user-side and spring side differential gears, and the braking system, respectively, yields:

$$\eta_u\dot{\theta}_u\tau_u + \eta_s\dot{\theta}_s\tau_s + \eta_b\dot{\theta}_b\tau_b = 0. \tag{5}$$

Combining the torque balance in the differential $\tau_u + \tau_s + \tau_b = 0$ with (5), and by postulating that the efficiency in the

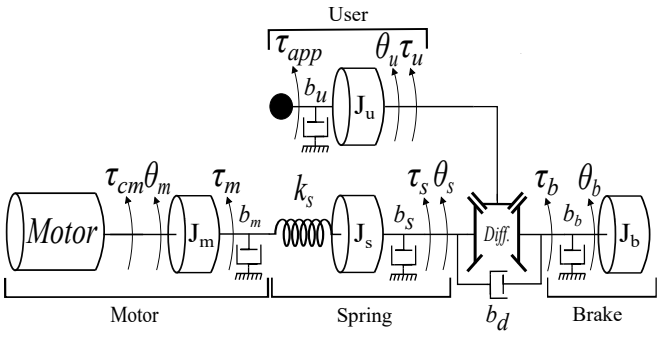

Fig. 3. DC-SEA Dynamics

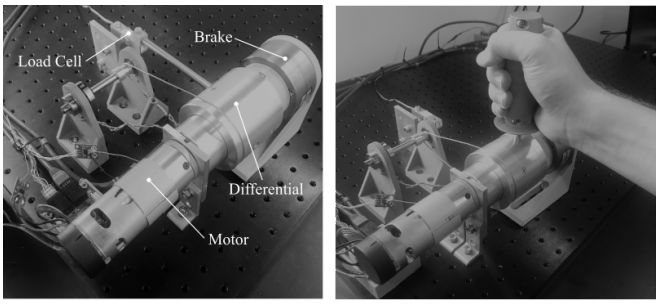

(a) DC-SEA Scenario 1 (b) DC-SEA Scenario 2

Fig. 4. Experimental setup: (a) Scenario 1: Measuring torque from the load cell with static output housing. (b) Scenario 2: Measuring torque from the inferred spring deflection with variable user position.

system is to be ideal, results in a set of split torque equations $\tau_s = \tau_b = \frac{\tau_u}{2}$, which combined with (2) to (4) provide:

$$(J_u+4J_s)\ddot{\theta}_u - 2J_s\ddot{\theta}_b + (b_u+4b_s+4b_d)\dot{\theta}_u - (2b_s+4b_d)\dot{\theta}_b - 2k_s\theta_m + 4k_s\theta_u - 2k_s\theta_b = \tau_{app} \quad (6)$$

and:

$$-2J_s\ddot{\theta}_u + (J_b+J_s)\ddot{\theta}_b - (2b_s+4b_d)\dot{\theta}_u + (b_b+b_s+4b_d)\dot{\theta}_b + k_s\theta_m - 2k_s\theta_u + k_s\theta_b = \tau_{cb} \quad (7)$$

Taking into consideration that J_u, J_m, and J_b are dominating inertial components and b_d, b_m, and b_b are the most prominent frictional components in the actuator, the remaining inertia, friction, and other dynamic losses can be neglected. The resulting equations of motion from (1), (6), and (7) become:

$$J_m\ddot{\theta}_m + b_m\dot{\theta}_m + k_s\Delta\theta_s = \tau_{cm} \quad (8)$$

$$J_u\ddot{\theta}_u + 4b_d\dot{\theta}_u - 4b_d\dot{\theta}_b - 2k_s\Delta\theta_s = \tau_{app} \quad (9)$$

$$J_b\ddot{\theta}_b - 4b_d\dot{\theta}_u + (4b_d+b_b)\dot{\theta}_b + k_s\Delta\theta_s = \tau_{cb}, \quad (10)$$

where $\Delta\theta_s = \theta_m - 2\theta_u + \theta_b$ is the deflection of the spring. Therefore, by controlling the deflection of the elastic element in the actuator, one can actively control the amount of torque delivered to the user, i.e., τ_{app}.

A. Free Motion

In this mode, θ_m is zero under the assumption that a motor with a large gear reduction is used in the actuator, where any reasonable amount of torque provided by the user will not cause the motor shaft to rotate. Thus, one can assume that when the motor is disengaged, its position remains constant. Due to the gearing in the differential, the angular position of the brake can be approximated to be twice that of the output shaft, i.e., $\theta_b \approx 2\theta_u$. The actuator inertia and viscous frictional components do cause a small deflection in the spring and, therefore, combining (9) and (10) to produce τ_{app} as a function of θ_u:

$$\tau_{app} = (J_u + 4J_b)\ddot{\theta}_u + (4b_d + 4b_b)\dot{\theta}_u, \quad (11)$$

showing that the torque experienced by the user stems from the inertia and viscous friction in the output housing and brake bodies of the differential.

B. Elastic Mode

When the motor is disengaged ($\theta_m = 0$) and the brake is fully engaged ($\theta_b = 0$), this mode fully engages the differential clutch and, therefore, nearly all energy introduced by the user is transferred to the spring. This can be shown in (9) by:

$$\tau_{app} = J_u\ddot{\theta}_u + 4b_d\dot{\theta}_u + 4k_s\theta_u \quad (12)$$

C. Active and Resistive Mode

Active mode and resistive mode can be achieved by adjusting motor torque τ_{cm} and braking torque τ_{cb}. When these modes are desired, τ_{cm} and τ_{cb} work in tandem to produce, reduce, or maintain the torque stored in the spring. The resultant torque felt by the user can be approximated to be twice the torque stored in the spring due to the differential gear ratio. The motor is used to compress the spring and engage the output shaft, where the brake provides a means of quickly and efficiently dissipating any unwanted energy introduced in the system. The equations of motion used for the actuator to follow a reference torque $\tau_{app} = \tau_{ref}$ is:

$$\tau_{ref} = J_u\ddot{\theta}_u + 4b_d\dot{\theta}_u - 4b_d\dot{\theta}_b - 2k_s\Delta\theta_s, \quad (13)$$

where either:

$$k_s\Delta\theta_s = \begin{cases} \tau_{cm} - J_m\ddot{\theta}_m - b_m\dot{\theta}_m, & \text{if } k_s\Delta\theta_s < \tau_{ref}/2 \\ \tau_{cb} - J_b\ddot{\theta}_b + 4b_d\dot{\theta}_u - (4b_d+b_b)\dot{\theta}_b, & \text{otherwise} \end{cases} \quad (14)$$

can be used to reach the reference torque, provided that τ_{cm} and τ_{cb} are operating within the rated motor and brake torques, respectively. The first line in the above equation corresponds to the condition in which there is not sufficient torque in the spring. Since the brake is not able to provide any energy to the system, the commanded motor torque must be increased. The difference between active and resistive modes lies within the direction of the force provided to the user. Active or assistive mode applies a torque in the same direction as a particular angular positional goal, while resistive mode counteracts the motion of the user and attempts to hinder the user in reaching a particular goal. For active mode, the motor must be engaged as the brake has no way of providing energy to the user. When resistive mode is required, the bulk of the load is dissipated by the

brake, increasing efficiency. By measuring the deflection in the spring, the required torques for both active and resistive modes can be achieved and maintained according to a professional therapist's recommendation.

IV. Experimental Results

The prototype of the DC-SEA and the experimental setup used to validate the model are shown in Fig. 4. Two experimental scenarios are tested.

In **Scenario 1** (Fig. 4(a)), a handle is attached to the output housing which is then rigidly connected to a load cell to measure output torque. The load cell measurement point is located at the same height as the central axis with a perpendicular distance of 150 mm. The angular position of the output shaft is fixed to characterize the actuator and validate the model.

In **Scenario 2** (Fig. 4(b)), the user rotates the output shaft while the actuator attempts to maintain a reference output torque pattern, as will be shown, this is equivalent to maintaining a deflection in the spring.

A. Characterization and Model Identification

The first experiment was ran in Scenario 1 to identify model parameters including stiffness of the spring. In this experiment, the motor was commanded to run at a constant velocity while the current of the brake was ramped from 0 A to 0.1 A and then back to 0 A following the temporal signal shown in Fig. 5(a). The measured and filtered output torque as a function of the brake current is shown in Fig. 5(b). The results obtained in Fig. 5(b) indicate a non-linear relation between the output torque and the brake current. This is due to the magnetic saturation of the brake and its magnetic hysteresis. The resultant measured spring deflection from this experiment is shown in Fig. 5(c). Furthermore, it can be seen in Fig. 5(c) the stiffness of the custom-made spring is non-linear and the effects of the magnetic hysteresis become more prominent. From this experiment, the stiffness of the spring in the linear range is estimated to be $k_s = 0.56$ Nm/rad.

The inertia in the different differential bodies was calculated analytically to be $J_u = 3.75$ kg·m^2, $J_b = 0.25$ kg·m^2, and $J_m = 0.20$ kg·m^2. The viscous friction was determined to be $b_d = 0.2$ Nm·s in the differential gears, $b_m = 0.1$ Nm·s in the motor, and $b_b = 0.1$ Nm·s in the brake.

B. Model Validation

This experiment, also run in Scenario 1, is used to show the accuracy of the model. In the experiment, the actuator was commanded to follow a square reference signal with a period of 8 seconds and a duty cycle of 50% with an amplitude of 1.5 Nm. In this experiment, the motor was open-loop controlled by providing a reference voltage and the current of the brake was used as the closed-loop control input. The spring used for this experiment had a constant of $k_s = 1.7$ Nm/rad. The parameters of the previous experiment, with the exception of the spring, were input into the model to estimate the required brake current to follow the desired output torque. A PID controller was used to regulate the brake current as shown in the block diagram in Fig. 6 (Scenario 1). The simulated and experimental results are shown in Fig. 7.

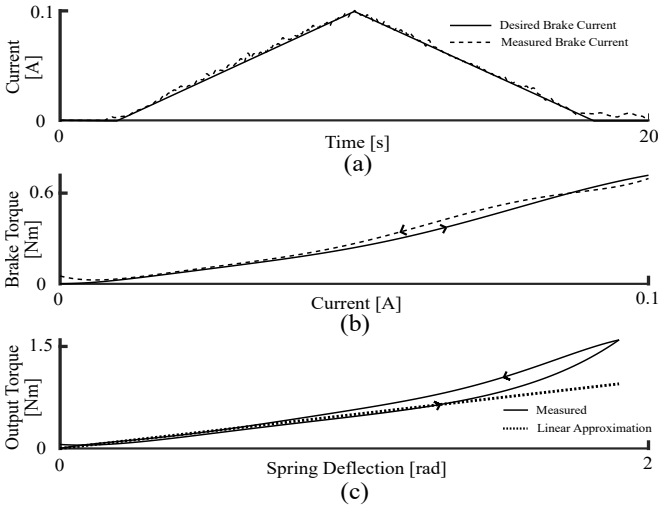

Fig. 5. Experimental results in Scenario 1. The motor is commanded to run at a constant velocity while the current of the brake follows a curve shown in (a). The resultant braking torque as a function of the brake current is shown in (b). In (c), the actuator's output torque as a function of the measured spring deflection is shown, from which the spring constant can be estimated.

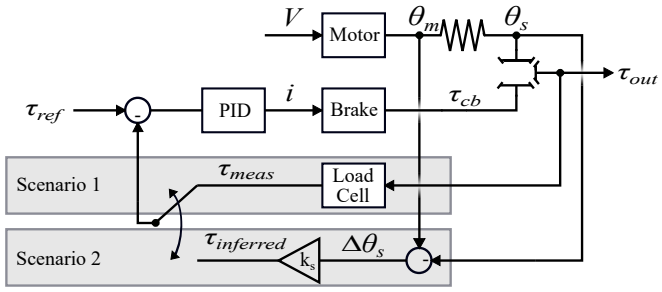

Fig. 6. Block diagram of the control loops used to regulate the brake current in Scenarios 1 and 2. In Scenario 1, the output torque is directly obtained from the load cell measurements, whereas in Scenario 2, the output torque is inferred from the deflection in the spring.

Fig. 7(a) shows the simulated and measured output torque response. The simulated output torque represents the torque estimated using the same model parameters and PID controller gains as the experiment. Also shown in Fig. 7(a), the output torque can be inferred from the spring by multiplying the measured spring deflection to the estimated spring constant from the previous experiment. Both the simulated and spring-inferred output torques show agreement with the measured output torque. The accuracy of the model can be confirmed by noticing that the simulated and measured brake current follow a trend as shown in Fig. 7(b). Fig. 7(c) shows the spring deflection measured from the experiment.

C. Torque Control Through Spring Deflection

From the previous experiments, it is confirmed that the output torque can be accurately represented by the deflection of the spring provided that the spring is operating within its linear range. Turning the focus to Scenario 2 (Fig. 4(b)), the

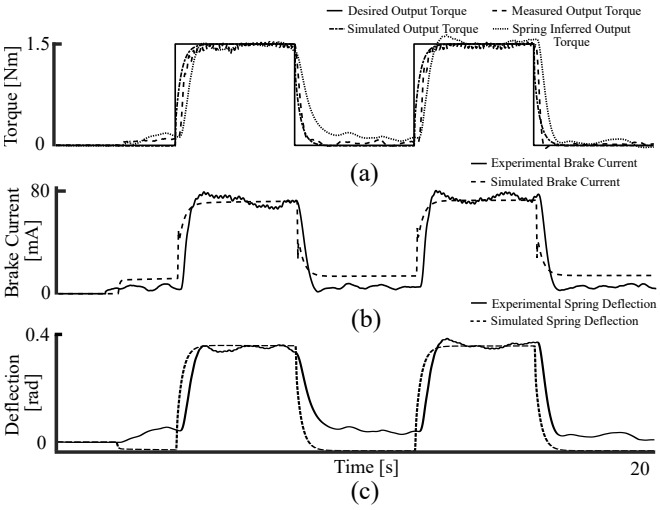

Fig. 7. Experimental results in Scenario 1. (a) shows the actuator's responce to a reference torque along with the simulated results. (a) also shows the spring inferred output torque based on the spring constant and measured deflection. In (b), the simulated and measured brake current that is required to follow a reference torque is shown. (c) shows the measured and simulated deflection of the spring.

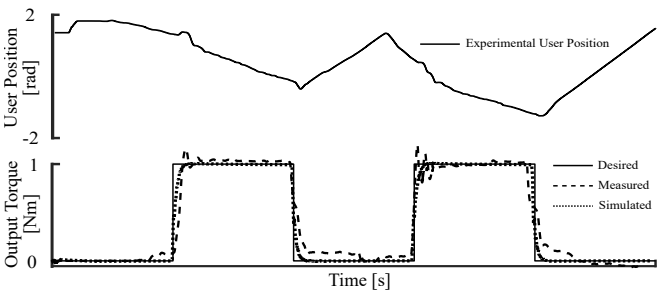

Fig. 8. Experimental results in Scenario 2. The top illustrates the measured user position. The bottom shows the desired, measured, and simulated output torque obtained based on the deflection of the spring and estimated stiffness.

objective now is to adhere to a specific reference torque as a user manipulates the output shaft.

A PID controller, as illustrated in Fig. 6, was implemented to maintain a specified output torque by controlling the deflection in the spring. Provided a reference torque τ_{ref}, the required spring deflection can be determined by: $\Delta\theta_s = \tau_{ref}/2k_s$ where $\tau_{ref} = 1$ Nm is the desired reference torque. The simulated and experimental results are shown in Fig. 8.

Fig. 8 (top) presents the measured angular position of the output shaft. Fig. 8 (bottom) illustrates the measured and simulated response of the actuator to a reference torque signal. As can be seen in the figure, the actuator was able to achieve the required spring deflection to maintain the reference output torque. The response shown in Fig. 8 (bottom) makes use of the spring deflection as a way to infer the output torque experienced by the user.

D. Discussion

The experiments showed the validity of the DC-SEA to provide reasonably accurate torque control. There are three methods to control the output torque. In the first method, the motor is open-loop controlled to introduce energy to the actuator while the output torque can be controlled by adjusting the current in the brake. When a motor with a high gear reduction is used, this provides a faster response and the output torque can be accurately inferred by measuring the compression in the torsion spring. Accurate characterization of the system is crucial since non-linear effects in the spring constant, magnetic hysteresis of the brake, and viscous and static friction can strongly affect the accuracy of the model and hence that of the controller. The second method, which is not presented in this paper, relies on fully engaging the brake and controlling the deflection of the spring through the motor as in a conventional SEA. The third method makes use of closed-loop control of the motor and brake torques in tandem to provide optimal control performance in more complex reference torque patterns, such as a sudden directional change in an output torque. The proposed design allows for any of the three control methods to be used, offering a greater level of control over traditional SEAs.

The increased versatility of the actuator does come at a cost. The addition of a differential clutch increases the complexity of the mechanical design. Some notable disadvantages of the differential clutch include friction losses between the satellite and planetary gears, additional inertia, and potential backlash between the differential gear teeth.

V. Conclusions and Future Work

This paper introduced a proof-of-concept differentially-clutched series elastic actuator (DC-SEA) to be used for musculoskeletal rehabilitation. The main goal of the DC-SEA is to encompass the performance requirements for differing phases of musculoskeletal rehabilitation while ensuring safety through hardware compliance. The concept consists of a brake connected to a motor-spring assembly through a differential clutch. The clutch allows both devices and the output shaft to rotate at different speeds. The proposed design adds to the functionality of classical series elastic actuators and is able to reproduce the operation capabilities of a range of preexisting elastic actuators.

A dynamic model of the proposed actuator was developed and tested in two different experimental scenarios. A simple torque control method was implemented to show that the output torque of the actuator can follow a specific reference dynamically by measuring the deflection of a spring. In future work, robust control methods will be explored to account for all nonlinearities caused by the spring, static friction, and the magnetic hysteresis in the particle brake.

The proposed actuator will be implemented in a home-based rehabilitation regime to assist patients with musculoskeletal disorders under the direct supervision of a clinician. Having access to rehabilitative devices at home could decrease recovery time and also allow therapists to take on a larger number of patients.

References

[1] A. Bicchi and G. Tonietti, "Fast and" soft-arm" tactics [robot arm design]," *IEEE Robotics & Automation Magazine*, vol. 11, no. 2, pp. 22–33, 2004.

[2] H. Vallery, J. Veneman, E. Van Asseldonk, R. Ekkelenkamp, M. Buss, and H. Van Der Kooij, "Compliant actuation of rehabilitation robots," *IEEE Robotics & Automation Magazine*.

[3] C. Rossa, J. Lozada, and A. Micaelli, "Design and control of a dual unidirectional brake hybrid actuation system for haptic devices," *IEEE Transactions on Haptics*, vol. 7, no. 4, pp. 442–453, Oct 2014.

[4] S. Zhang, S. Guo, Y. Fu, L. Boulardot, Q. Huang, H. Hirata, and H. Ishihara, "Integrating compliant actuator and torque limiter mechanism for safe home-based upper-limb rehabilitation device design," *Journal of Medical and Biological Engineering*, vol. 37, no. 3, pp. 357–364, 2017.

[5] G. A. Pratt and M. M. Williamson, "Series elastic actuators," *Intelligent Robots and Systems 95.'Human Robot Interaction and Cooperative Robots', Proceedings. 1995 IEEE/RSJ International Conference on*, vol. 1, pp. 399–406, 1995.

[6] P. Maciejasz, J. Eschweiler, K. Gerlach-Hahn, A. Jansen-Troy, and S. Leonhardt, "A survey on robotic devices for upper limb rehabilitation," *Journal of neuroengineering and rehabilitation*, vol. 11, no. 1, p. 3, 2014.

[7] A. J. Veale and S. Q. Xie, "Towards compliant and wearable robotic orthoses: A review of current and emerging actuator technologies," *Medical engineering & physics*, vol. 38, no. 4, pp. 317–325, 2016.

[8] N. Nordin, S. Q. Xie, and B. Wünsche, "Assessment of movement quality in robot-assisted upper limb rehabilitation after stroke: a review," *Journal of neuroengineering and rehabilitation*, vol. 11, p. 137, 2014.

[9] H. Yu, S. Huang, G. Chen, Y. Pan, and Z. Guo, "Human–robot interaction control of rehabilitation robots with series elastic actuators," *IEEE Transactions on Robotics*, vol. 31, no. 5, pp. 1089–1100, 2015.

[10] N. T. Pham, N. D. K. Nguyen, T. T. Nguyen, S. B. Kim *et al.*, "Development of series elastics actuators for physical rehabilitation devices," in *International Conference on Advanced Engineeringá Theory and Applications*. Springer, 2016, pp. 702–712.

[11] A. Hochstenbach-Waelen and H. A. Seelen, "Embracing change: practical and theoretical considerations for successful implementation of technology assisting upper limb training in stroke," *Journal of neuroengineering and rehabilitation*, vol. 9, no. 1, p. 52, 2012.

[12] S.-S. Yoon, S. Kang, S.-k. Yun, S.-J. Kim, Y.-H. Kim, and M. Kim, "Safe arm design with mr-based passive compliant joints and viscoelastic covering for service robot applications," *Journal of mechanical science and technology*, vol. 19, no. 10, pp. 1835–1845, 2005.

[13] N. Paine, S. Oh, and L. Sentis, "Design and control considerations for high-performance series elastic actuators," *IEEE/ASME Transactions on Mechatronics*, vol. 19, no. 3, pp. 1080–1091, 2014.

[14] K. Kong, J. Bae, and M. Tomizuka, "A compact rotary series elastic actuator for human assistive systems," *IEEE/ASME transactions on mechatronics*, vol. 17, no. 2, pp. 288–297, 2012.

[15] J. P. Cummings, D. Ruiken, E. L. Wilkinson, M. W. Lanighan, R. A. Grupen, and F. C. Sup, "A compact, modular series elastic actuator," *Journal of Mechanisms and Robotics*, vol. 8, no. 4, p. 041016, 2016.

[16] S. Oh and K. Kong, "High-precision robust force control of a series elastic actuator," *IEEE/ASME Transactions on Mechatronics*, vol. 22, no. 1, pp. 71–80, 2017.

[17] H.-C. Hsieh, D.-F. Chen, L. Chien, and C.-C. Lan, "Design of a parallel actuated exoskeleton for adaptive and safe robotic shoulder rehabilitation," *IEEE/ASME Trans. Mechatronics*, vol. 22, no. 5, pp. 2034–2045, 2017.

[18] E. Sariyildiz, G. Chen, and H. Yu, "A unified robust motion controller design for series elastic actuators," *IEEE/ASME Transactions on Mechatronics*, vol. 22, no. 5, pp. 2229–2240, 2017.

[19] D. W. Robinson, "Design and analysis of series elasticity in closed-loop actuator force control," Ph.D. dissertation, Massachusetts Institute of Technology, 2000.

[20] A. Calanca and P. Fiorini, "Understanding environment-adaptive force control of series elastic actuators," *IEEE/ASME Transactions on Mechatronics*, vol. 23, no. 1, pp. 413–423, 2018.

[21] H. Yu, S. Huang, G. Chen, and N. Thakor, "Control design of a novel compliant actuator for rehabilitation robots," *Mechatronics*, vol. 23, no. 8, pp. 1072–1083, 2013.

[22] M. Lauria, M.-A. Legault, M.-A. Lavoie, and F. Michaud, "Differential elastic actuator for robotic interaction tasks," in *Robotics and Automation, IEEE International Conference on*. IEEE, 2008, pp. 3606–3611.

[23] F. Conti and O. Khatib, "A new actuation approach for haptic interface design," *The International Journal of Robotics Research*, vol. 28, no. 6, pp. 834–848, 2009.

[24] B. Chen, X. Zhao, H. Ma, L. Qin, and W.-H. Liao, "Design and characterization of a magneto-rheological series elastic actuator for a lower extremity exoskeleton," *Smart Materials and Structures*, vol. 26, no. 10, p. 105008, 2017.

[25] U. Mettin, P. X. La Hera, L. B. Freidovich, and A. S. Shiriaev, "Parallel elastic actuators as a control tool for preplanned trajectories of underactuated mechanical systems," *The international journal of robotics research*, vol. 29, no. 9, pp. 1186–1198, 2010.

[26] R. Alexander, "Three uses for springs in legged locomotion," *International Journal of Robotics Research*, vol. 9, no. 2, pp. 53–61, 1990.

[27] D. F. Häufle, M. Taylor, S. Schmitt, and H. Geyer, "A clutched parallel elastic actuator concept: Towards energy efficient powered legs in prosthetics and robotics," pp. 1614–1619, 2012.

[28] M. Plooij, G. Mathijssen, P. Cherelle, D. Lefeber, and B. Vanderborght, "Lock your robot: A review of locking devices in robotics," *IEEE Robotics & Automation Magazine*, vol. 22, no. 1, pp. 106–117, 2015.

[29] E. J. Rouse, L. M. Mooney, and H. M. Herr, "Clutchable series-elastic actuator: Implications for prosthetic knee design," *The International Journal of Robotics Research*, vol. 33, no. 13, pp. 1611–1625, 2014.

[30] M. Plooij, W. Wolfslag, and M. Wisse, "Clutched elastic actuators," *IEEE/ASME Transactions on Mechatronics*, vol. 22, no. 2, pp. 739–750, 2017.

[31] M. Plooij, M. Wisse, and H. Vallery, "Reducing the energy consumption of robots using the bidirectional clutched parallel elastic actuator," *IEEE Transactions on Robotics*, vol. 32, no. 6, pp. 1512–1523, 2016.

[32] D. Chapuis, X. Michel, R. Gassert, C.-M. Chew, E. Burdet, and H. Bleuler, "A haptic knob with a hybrid ultrasonic motor and powder clutch actuator," pp. 200–205, 2007.